

Draft processed October 30, 2018

## Detection of Far-Infrared Water Vapor, Hydroxyl, and Carbon Monoxide Emissions from the Supernova Remnant 3C 391 <sup>1</sup>

William T. Reach<sup>1</sup>

Infrared Processing and Analysis Center, California Institute of Technology, Pasadena, CA 91125

Jeonghee Rho<sup>2</sup>

Service d'Astrophysique, CEA, DSM, DAPNIA, Centre d'Etudes de Saclay, F-91191 Gif-sur-Yvette cedex, France

### ABSTRACT

We report the detection of shock-excited far-infrared emission of H<sub>2</sub>O, OH, and CO from the supernova remnant 3C 391, using the *ISO* Long-Wavelength Spectrometer. This is the first detection of thermal H<sub>2</sub>O and OH emission from a supernova remnant. For two other remnants, W 28 and W 44, CO emission was detected but OH was only detected in absorption. The observed H<sub>2</sub>O and OH emission lines arise from levels within  $\sim 400$  K of the ground state, consistent with collisional excitation in warm, dense gas created after the passage of the shock front through the dense clumps in the pre-shock cloud. The post-shock gas we observe has a density  $\sim 2 \times 10^5$  cm<sup>-3</sup> and temperature 100–1000 K, and the relative abundances of CO:OH:H<sub>2</sub>O in the emitting region are 100:1:7 for a temperature of 200 K. The presence of a significant column of warm H<sub>2</sub>O suggests that the chemistry has been significantly changed by the shock. The existence of significant column densities of both OH and H<sub>2</sub>O, which is at odds with models for non-dissociative shocks into dense gas, could be due to photodissociation of H<sub>2</sub>O or a mix of fast and slow shocks through regions with different pre-shock density.

*Subject headings:* supernova remnants – Infrared: interstellar: lines – ISM: molecules – ISM: individual (3C 391)

### 1. Introduction

Long suspected to be an important component of the interstellar medium, water has proven difficult to observe because of the dominating absorption by water vapor in the Earth's atmosphere. Water masers at radio frequencies are bright enough to penetrate the atmosphere, but they are rare and their physical conditions may be exceptional. Now that we have flown a sensitive infrared spectrometer in space, aboard the *Infrared Space Observatory* (Kessler et al. 1996), transitions among energy levels  $\sim 100$ –1000 K

---

<sup>1</sup>Based on observations with ISO, an ESA project with instruments funded by ESA Member States (especially the PI countries: France, Germany, the Netherlands and the United Kingdom) with the participation of ISAS and NASA.

<sup>1</sup>formerly Institut d'Astrophysique Spatiale, Bâtiment 121, Université Paris XI, 91405 Orsay cedex, France

<sup>2</sup>postal address: Physics Department, University of California, Santa Barbara, CA 93106

above the ground state of H<sub>2</sub>O are observable. Early results from *ISO* indicate that H<sub>2</sub>O is a significant constituent in a cloud near the galactic center (Cernicharo et al. 1997) and that H<sub>2</sub>O is as abundant as CO in shocked regions in Orion (Harwit et al. 1998).

The observations reported here are part of a study of the infrared emission from supernova remnants interacting with molecular clouds. Our targets were selected from a sample of supernova remnants with previous evidence for interaction with nearby molecular clouds based on X-ray and radio morphology (Rho & Petre 1998), millimeter-wave molecular line observations (Wilner et al. 1998, Wootten 1977, Wootten 1981, Reach and Rho 1998), and OH 1720 MHz observations (Frail et al. 1996, Green et al. 1997). The presence of 1720 MHz maser emission without bright main-line OH maser emission suggests that they are collisionally excited (Elitzur 1976), and their location in bright radio remnants indicates that they are produced in the dense regions just behind molecular shocks. The first results of our *ISO* observations showed that the [O I] 63  $\mu$ m line, which is expected to be one of the brightest cooling lines for post-shock gas for a wide range of gas densities and shock velocities, is very bright at the locations of the OH masers (Reach and Rho 1996; Paper I). In a parallel observational project, we also found shock-accelerated CS, CO, and HCO<sup>+</sup> molecules in 3C 391 (Reach and Rho 1998). In this paper, we present follow-up spectral observations to see which additional infrared lines are bright from molecular supernova shocks. These observations are the first detection of far-infrared H<sub>2</sub>O, OH, and CO lines from supernova remnants. We report here far-infrared spectral observations of a single position in each of 3 supernova remnants: 3C 391, W 44, and W 28.

## 2. Observations

All observations reported here were performed with the *ISO* Long-Wavelength Spectrometer (Clegg et al. 1996). We used the medium-resolution grating to fully sample the wavelength range from 42.2–188.6  $\mu$ m. The coordinates are based on bright OH 1720 MHz masers (Frail et al. 1996) in each remnant (for W 44: 18<sup>h</sup>56<sup>m</sup>28.4<sup>s</sup> +01°29'59", for W 28: 18<sup>h</sup>01<sup>m</sup>52.3<sup>s</sup> -23°19'25"; B1950); for 3C 391 we shifted closer to the peak of shocked CS and CO broad-molecular-line emission 3C 391:BML (18<sup>h</sup>46<sup>m</sup>47.1<sup>s</sup> -01°00'51") (Reach and Rho 1998). The LWS beamsize is 80", and the spectra are severely affected by fringes, due to constructive and destructive interference (inside the spectrometer) of wavefronts from our structured, extended sources. We removed the fringes using the *ISO* Spectral Analysis Package <sup>4</sup>, assuming that the emitting region is extended at all wavelengths.

An important portion of the spectrum of 3C 391:BML, including the low-lying transition of ortho-H<sub>2</sub>O at 179.5  $\mu$ m, is shown in Fig. 1. The continuum is due to dust from the supernova remnant (some 30% of the total) and unrelated interstellar material along the line of sight (see Paper I). In addition to the H<sub>2</sub>O and CO lines indicated, there are some remaining ripples in the spectrum that do not fall at the wavelength of predicted lines nor do they have the shape expected for an unresolved spectral line. A second spectral observation toward 3C 391:BML was performed in order to confirm some of the spectral lines, and to search for lines of H<sub>2</sub>O and OH from energy levels higher than we had already detected. The result for the OH ( $^2\Pi_{\frac{1}{2}-\frac{3}{2}}, J = \frac{1}{2} - \frac{3}{2}$ ) line is shown in Figure 2.

---

<sup>4</sup>The ISO Spectral Analysis Package (ISAP) is a joint development by the LWS and SWS Instrument Teams and Data Centres. Contributing institutes are CESR, IAS, IPAC, MPE, RAL and SRON.

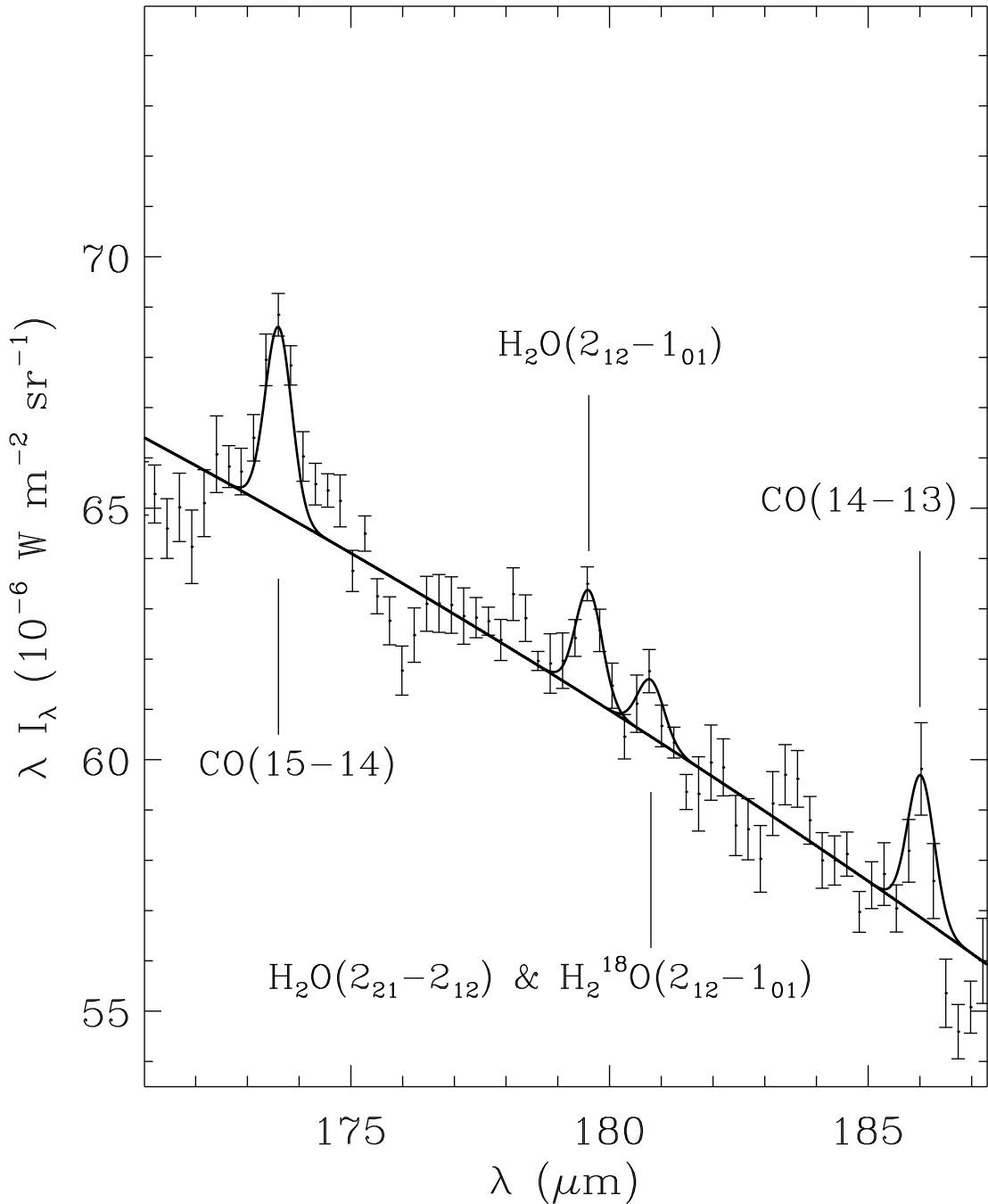


Fig. 1.— A portion of the far-infrared spectrum of 3C 391:BLM obtained the *ISO* LWS. The combination of a linear baseline and 4 lines (with the instrumental line profile) is shown as a solid curve. Two  $\text{H}_2\text{O}$  lines and two CO lines are labeled by species and transition.

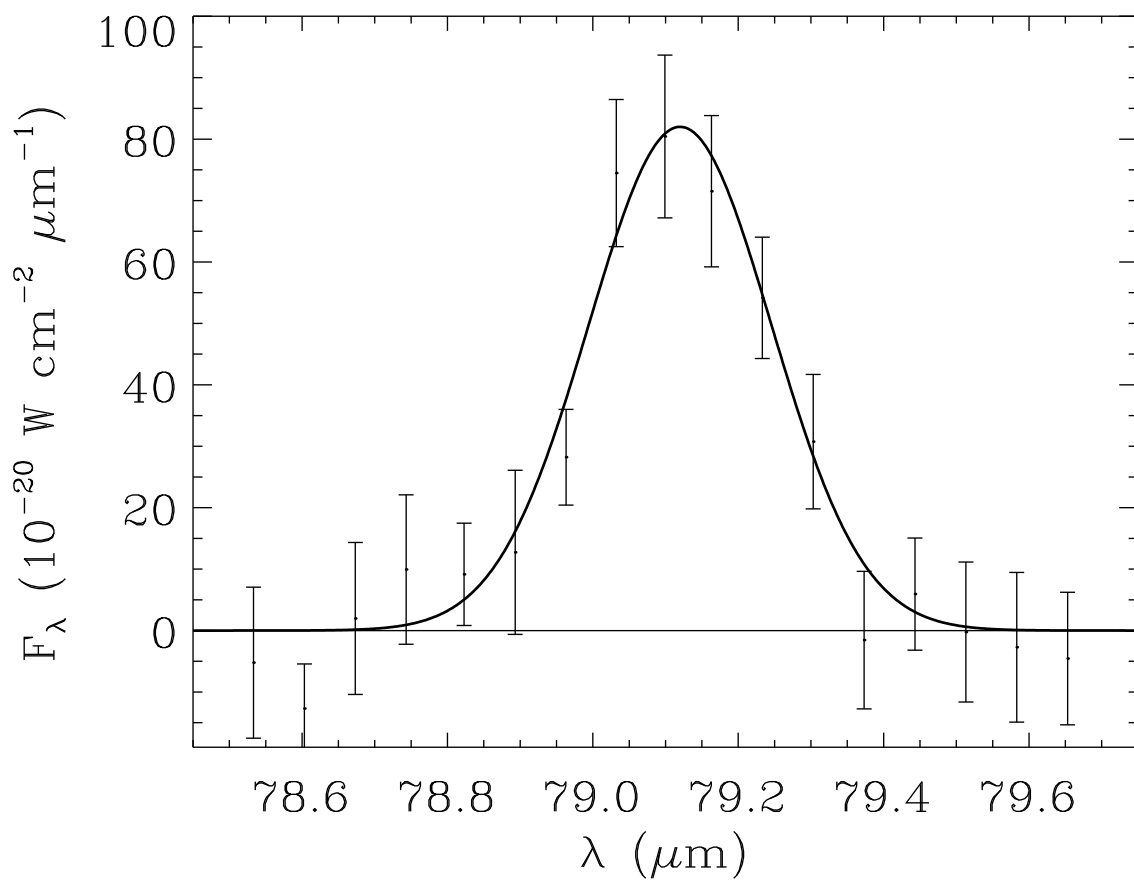


Fig. 2.— Spectrum of the OH [ ${}^2\Pi_{\frac{1}{2}}(J = \frac{1}{2}) - {}^2\Pi_{\frac{3}{2}}(J = \frac{3}{2})$ ] line for 3C 391: BML.

### 3. Results

Very bright lines from atomic and ionic C, N, and O, and weaker molecular lines were detected from all three supernova remnants. We will compile and present the complete line lists in a future paper. Of the three sources that we observed, only 3C 391:BML had a rich spectrum of molecular emission. A list of H<sub>2</sub>O, OH, and CO lines detected or limited toward 3C 391:BML is shown in Table 1. For W 28, the CO(16-15) and CO(15-14) emission lines were detected, and for W 44 only the CO(16-15) line was detected; the CO lines are a factor of 2 and 4 fainter for W 28 and W 44 compared to 3C 391:BML. The 95% confidence upper limit on the H<sub>2</sub>O(2<sub>12</sub>-1<sub>01</sub>) 179.5  $\mu\text{m}$  line for W 44 and W 28 is half the brightness of the line detected toward 3C 391:BML. Considering that 3C 391 also had the brightest [O I] 63  $\mu\text{m}$  line and dust continuum, it is possible that both W 28 and W 44 could have similar shock-excited spectra, with the H<sub>2</sub>O lines unfortunately just below our detection limit. While no OH emission was detected for W 28 and W 44, the 119  $\mu\text{m}$  transition from the ground-state was detected in *absorption*, presumably due to foreground gas. One source of uncertainty is the identification of the lines. Although the resolving power of these observations was less than 300, such that wavelengths cannot be measured sufficiently accurately for conclusive identifications, our main conclusion—namely, that H<sub>2</sub>O, OH, and CO were detected from shock-excited gas in supernova remnants—is strong. In the time-honored tradition of spectroscopy, we have detected multiple lines from each species.

All of the lines we believe we have detected are from the lowest accessible energy levels of each species. For CO, the highest level we detected was  $J = 16$ , which lies 750 K above the ground state. The energy level diagrams of H<sub>2</sub>O and OH are shown in Figures 3 and 4. In both cases, we indicate the fast transitions whose wavelengths fall within the range of our *ISO* spectrum. Including marginal detections, we see evidence for almost all of the fast transitions of both ortho and para H<sub>2</sub>O among energy levels within 320 K of the ground state. The H<sub>2</sub>O(4<sub>13</sub> – 3<sub>22</sub>) transition is masked by a bright [O I] line nearby, but there is a hint of the principal line from the next-highest energy level (3<sub>30</sub> – 2<sub>21</sub>). No transitions involving levels more than 400 K above ground are seen. The most important emission line that is expected to be bright but is not detected is the 119  $\mu\text{m}$  line of OH. But this line connects directly to the ground state, and our models (below) predict significant foreground absorption; therefore, we suspect that the 119  $\mu\text{m}$  line is extinguished by foreground gas. Indeed, our spectra of W 44 and W 28, which have comparable sightlines through the galactic disk, show absorption features at 119  $\mu\text{m}$  (with an optical depth of order 0.1) due to foreground OH absorbing the dust continuum from the supernova remnants.

### 4. Discussion

#### 4.1. Excitation and abundance of H<sub>2</sub>O, OH, and CO

In order to determine the physical conditions that can produce the observed suite of spectral lines, and to measure the abundances of the observed species, we compared the line brightnesses to a simple model that balances collisional and radiative transitions within a uniform emitting region. We modeled the emission spectra of regions with a range of H<sub>2</sub> volume density and kinetic temperature, and the absorption spectrum of a cold slab of foreground gas with nominal molecular abundances (from Irvine et al. 1987) and an H<sub>2</sub> column density of 10<sup>22</sup> cm<sup>-2</sup>. We solved iteratively for the excitation, modifying radiative rates by the escape probability for a line profile with a width of 30 km s<sup>-1</sup>, as was found from the millimeter-wave CS and CO observations (Reach and Rho 1998). Collision rates were taken from Offer, van Hemert, & van Dishoeck (1994) for OH and Green, Maluendes, & McLean (1993) for H<sub>2</sub>O, and the radiative transition

Table 1. Molecular Lines from 3C 391:BML

transition <sup>a</sup>	flux (nW m <sup>-2</sup> sr <sup>-1</sup> )	$\lambda$ <sup>b</sup> ( $\mu$ m)	SNR
CO (14-13)	9.0 $\pm$ 2.2	186.06	2.9
CO (15-14) <sup>c</sup>	28.8 $\pm$ 2.3	173.62	6.4
CO (16-15) <sup>c</sup>	10.0 $\pm$ 1.7	162.86	5.0
CO (17-16)	10.3 $\pm$ 2.8	153.51	3.0
CO (18-17) <sup>c</sup>	< 17	144.78	...
CO (19-18)	< 17	137.20	...
CO (20-19)	< 7	130.37	...
H <sub>2</sub> O (4 <sub>13</sub> -4 <sub>04</sub> )	< 8	187.11	...
H <sub>2</sub> <sup>18</sup> O (2 <sub>12</sub> -1 <sub>01</sub> ) <sup>c,d</sup>	6.6 $\pm$ 1.6	180.69	3.1
H <sub>2</sub> O (2 <sub>12</sub> -1 <sub>01</sub> )	10.0 $\pm$ 0.9	179.59	8.2
H <sub>2</sub> O (3 <sub>03</sub> -2 <sub>12</sub> ) <sup>c</sup>	6.3 $\pm$ 3.0	174.54	2.9
H <sub>2</sub> O (3 <sub>13</sub> -2 <sub>02</sub> )	< 13	138.53	...
H <sub>2</sub> O (4 <sub>23</sub> -4 <sub>14</sub> )	< 7	132.41	...
H <sub>2</sub> O (4 <sub>04</sub> -3 <sub>13</sub> )	< 13	125.35	...
H <sub>2</sub> O (4 <sub>14</sub> -3 <sub>03</sub> )	< 5	113.54	...
H <sub>2</sub> O (2 <sub>21</sub> -1 <sub>10</sub> )	< 7	108.07	...
H <sub>2</sub> O (2 <sub>20</sub> -1 <sub>11</sub> ) <sup>c</sup>	7.1 $\pm$ 2.0	100.47	2.9
H <sub>2</sub> O (5 <sub>15</sub> -4 <sub>04</sub> )	< 6	95.63	...
H <sub>2</sub> O (3 <sub>22</sub> -2 <sub>11</sub> )	< 7	89.99	...
H <sub>2</sub> O (3 <sub>21</sub> -2 <sub>12</sub> )	< 8	75.38	...
OH (1-1;3-1) <sup>c</sup>	4.2 $\pm$ 1.2	163.65	2.6
OH (3-3;5-3)	< 7	119.33	...
OH (1-3;5-7)	< 13	115.22	...
OH (1-1;5-3)	3.6 $\pm$ 1.4	98.69	2.6
OH (1-3;3-5)	< 9	96.34	...
OH (3-3;7-5)	12.7 $\pm$ 3.3	84.58	3.1
OH (1-3;1-3)	17.4 $\pm$ 1.9	79.11	11.9
OH (3-3;9-7)	< 13	65.20	...
OH (1-3;3-3)	< 13	53.30	...

<sup>a</sup>CO transitions are labeled in the format (*a*-*b*) where *a* and *b* are the upper and lower rotational quantum number; OH transitions are labeled in the format (*a*-*b*; *c*-*d*) indicating the transition from level  $^2\Pi_{a/2}$ , *J* = *c*/2 to level  $^2\Pi_{b/2}$ , *J* = *d*/2.

<sup>b</sup>Observed line center for detected lines, accurate to 0.2 (0.1)  $\mu$ m for  $\lambda$  greater (less) than 88  $\mu$ m; laboratory rest wavelength for undetected lines

<sup>c</sup>line potentially blended with another

<sup>d</sup>This line could be the H<sub>2</sub>O (2<sub>21</sub>-2<sub>12</sub>) transition instead, but the excitation model suggests this transition contributes less than 10% of the observed brightness.

rates were taken from Pickett et al. (1996). The observed brightness ratio of 79  $\mu\text{m}$  to 84  $\mu\text{m}$  lines of OH is sensitive to the gas density, suggesting  $n(\text{H}_2) \simeq (1 - 6) \times 10^5 \text{ cm}^{-3}$ . The ratios of the 5  $\rightarrow$  4, 3  $\rightarrow$  2, and 2  $\rightarrow$  1 millimeter lines of CS are also sensitive to the gas density, suggesting  $n(\text{H}_2) \simeq (3 - 4) \times 10^5 \text{ cm}^{-3}$ , and the millimeter CS and CO lines somewhat constrain the temperature,  $T > 50 \text{ K}$  (Reach and Rho 1998). For the abundance calculations, we will assume  $n(\text{H}_2) = 2 \times 10^5 \text{ cm}^{-3}$  and  $100 < T < 1000 \text{ K}$ , which is consistent with the presence and lack of other OH and  $\text{H}_2\text{O}$  lines in the observed wavelength range.

We determine the abundances of the various molecules assuming all lines arise from the same physical region, with constant temperature and density. The column density of OH is  $\sim 2 \times 10^{16} \text{ cm}^{-2}$ , and the optical depth of the 79  $\mu\text{m}$  line is of order unity. The CO excitation is much more sensitive to temperature; to match the brightness of the well-detected 15  $\rightarrow$  14 line, the CO column density  $\sim 2 \times 10^{18}(T/200)^{-5} \text{ cm}^{-2}$ . The  $\text{H}_2\text{O}$  lines are estimated to be optically thick: if we associate the line observed at 180.69  $\mu\text{m}$  with  $\text{H}_2^{18}\text{O}$  (2<sub>12</sub>-1<sub>10</sub>), then the isotope ratio implies an optical depth  $\sim 400$  for the brightest  $\text{H}_2\text{O}$  line. However, in the low-density limit,  $n(\text{H}_2) < 10^9 \text{ cm}^{-3}$ , spontaneous decay is still faster than collisional de-excitation, and the line brightness still measures the  $\text{H}_2\text{O}$  abundance (Irvine et al. 1987). The column density of  $\text{H}_2\text{O}$  from the excitation model is  $\sim 3 \times 10^{17} \text{ cm}^{-2}$ . To determine the absolute abundance of each species, we require a measure of the  $\text{H}_2$  column density. If we assume the emitting region is a uniform sphere with diameter equal to the observed angular size of shock-excited molecular gas ( $\sim 30''$  from Reach and Rho 1998), and we take from the excitation model  $n(\text{H}_2) = 2 \times 10^5 \text{ cm}^{-3}$ , we find  $N(\text{H}_2) \sim 8 \times 10^{23} \text{ cm}^{-3}$ . This value of  $N(\text{H}_2)$  agrees with the observed brightness (from our *ISO* SWS observations, in preparation) of the S(3) line of  $\text{H}_2$ , if  $T \simeq 200$ . In summary, we estimate the relative abundances of CO:OH: $\text{H}_2\text{O}$  to be 100:1:7, and the abundance of water in the shocked cloud is  $[\text{H}_2\text{O}/\text{H}_2] \sim 4 \times 10^{-7}$ .

#### 4.2. Chemistry of $\text{H}_2\text{O}$ and OH

The warm  $\text{H}_2\text{O}$  in 3C 391:BM is likely due to shock-enhanced chemistry. In relatively hot gas, OH is rapidly converted into  $\text{H}_2\text{O}$  by the reaction  $\text{OH} + \text{H}_2 \rightarrow \text{H}_2\text{O} + \text{H}$ , so that all the available O that is not already locked in CO would be converted into  $\text{H}_2\text{O}$  (Draine et al. 1983, McKee & Hollenbach 1979). Models for the oxygen chemistry predict very efficient conversion of OH into  $\text{H}_2\text{O}$  for non-dissociative shocks into high-density ( $n_0 = 10^5 \text{ cm}^{-3}$ ) clouds but comparable OH and  $\text{H}_2\text{O}$  column densities for shocks into intermediate-density ( $n_0 = 10^3 \text{ cm}^{-3}$ ) clouds, while CO and  $\text{H}_2\text{O}$  are comparably abundant (Graff & Dalgarno 1987). Behind a fully dissociative shock, the molecules re-form in a much cooler ( $\sim 100$ –500 K) region (Hollenbach & McKee 1989). In cooler gas, the 1420 K barrier (Wagner & Graff 1987) for the  $\text{OH} + \text{H}_2 \rightarrow \text{H}_2\text{O} + \text{H}$  reaction cannot be overcome, and OH is more abundant than  $\text{H}_2\text{O}$  (McKee & Hollenbach 1979, van Dishoeck and Black 1986) except deep inside dense molecular cores (Sternberg & Dalgarno 1995). The chemistry in cooler gas depends on photo-dissociation; OH is much more abundant than  $\text{H}_2\text{O}$  (van Dishoeck and Black 1986), except deep inside very dark cores, where the photodissociation rate is very low (Bergin et al. 1995).

The relative strengths of the  $\text{H}_2\text{O}$  lines that we observe were calculated by Kaufman & Neufeld (1996), and our observations are generally consistent with the models for pre-shock density  $n_0 = 10^{4-5} \text{ cm}^{-3}$ . However, these models predict a very low OH abundance: the  $\text{H}_2\text{O}$  179.5  $\mu\text{m}$  line is predicted to be two orders of magnitude brighter than the OH 84.5  $\mu\text{m}$  doublet, while we observe comparable brightnesses. The relatively low excitation we observe for the  $\text{H}_2\text{O}$  and OH molecules ( $T_{upper} < 400 \text{ K}$ ) suggests that the gas we are observing is not presently hot enough for the rapid  $\text{H}_2\text{O}$  production. But this does not preclude the  $\text{H}_2\text{O}$  having formed in a short-lived, high-temperature region, and we observe only the cooling region.

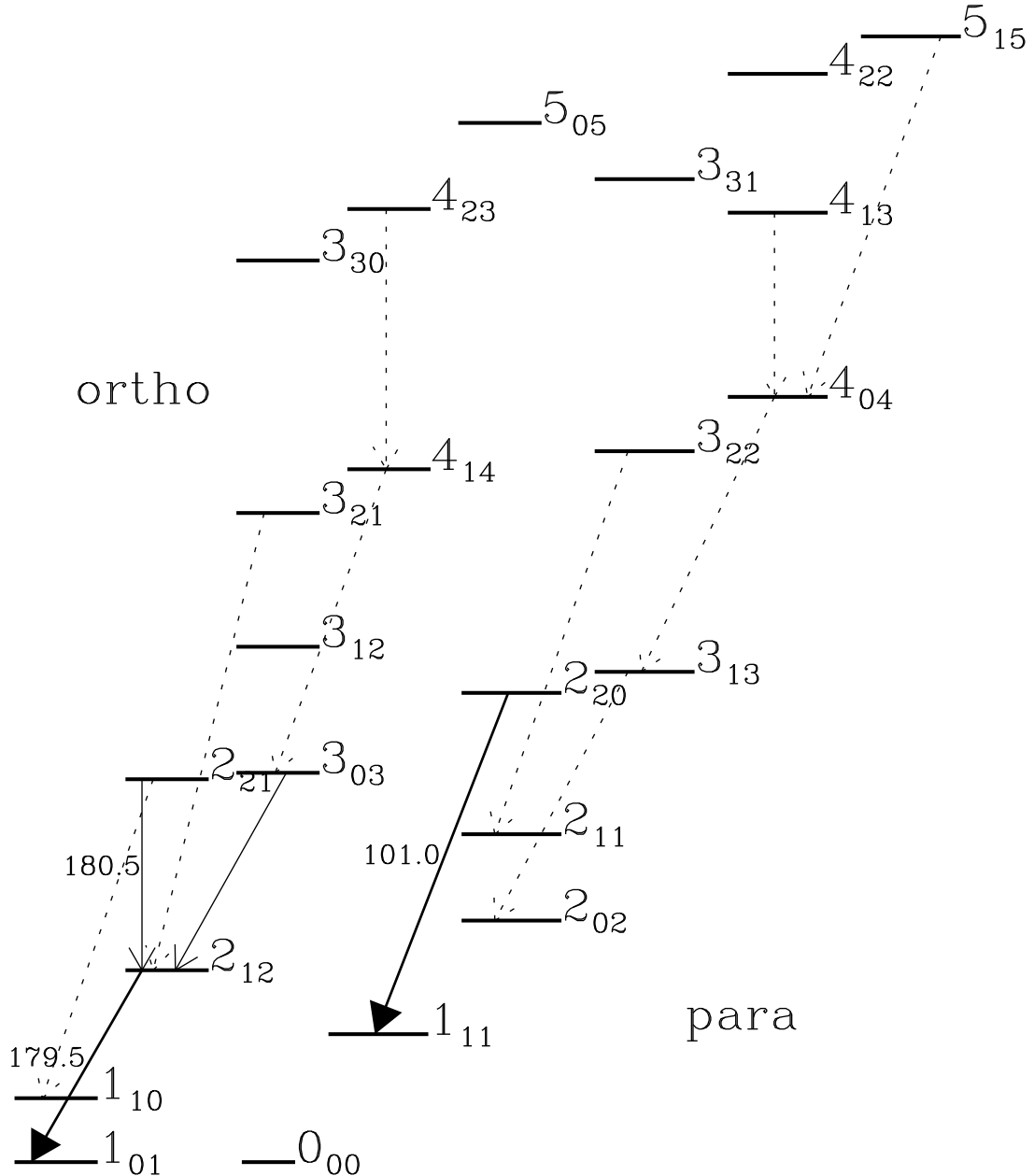


Fig. 3.— Energy-level diagrams for ortho (left) and para (right)  $\text{H}_2\text{O}$ . All levels within 500 K of the ground state are shown. The fastest radiative de-excitations of each level are indicated with arrows, if the wavelength of the transition is within the range of our *ISO* spectrum. The arrows were drawn with the following characteristics: detected lines have a solid-filled arrowhead, possible detections have an open arrowhead, and non-detections have dashed arrow.

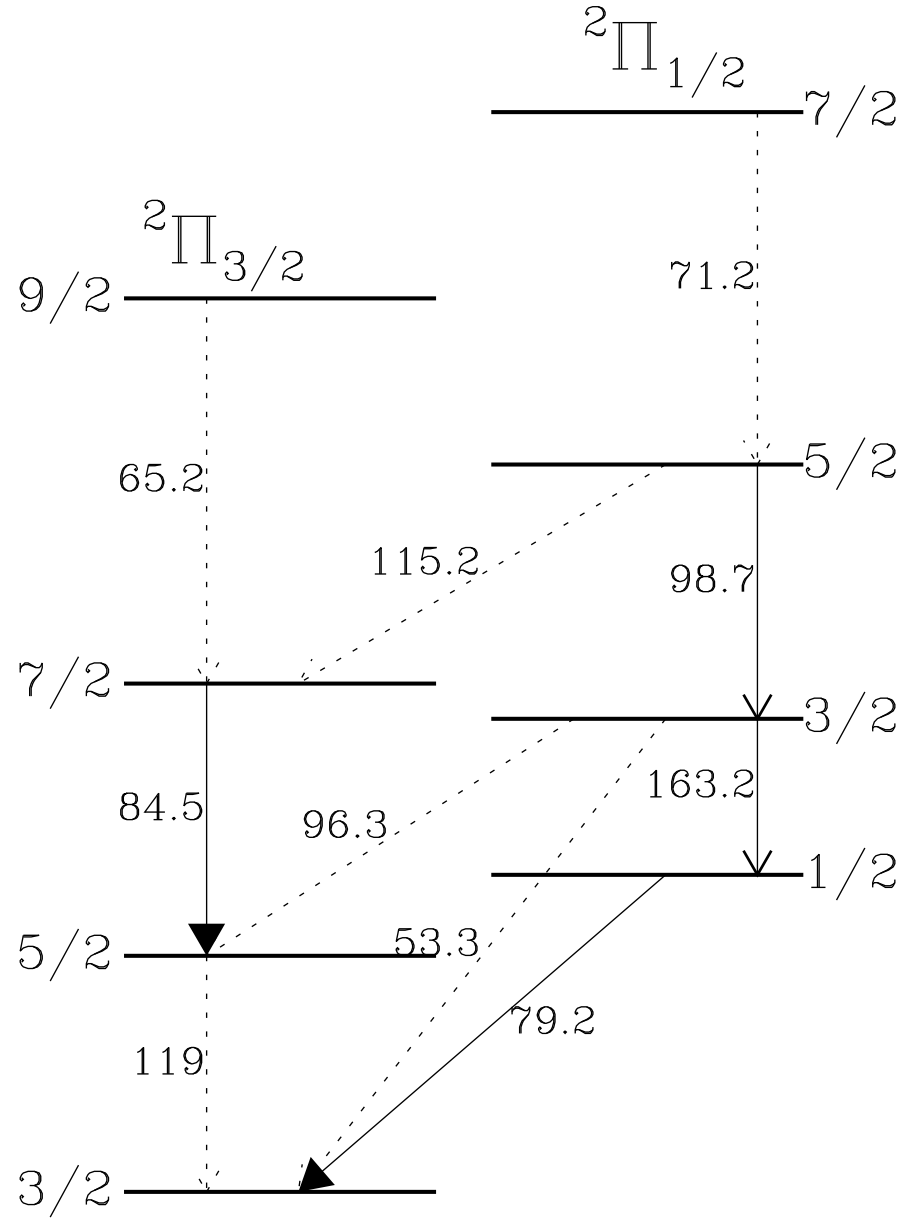


Fig. 4.— Energy-level diagram of OH. Each level is labeled by its rotational quantum number  $J$ . For the transitions within the range of our *ISO* spectrum, arrow symbols are the same as in Fig. 3. Clearly detected lines have a solid-filled arrowhead, possible detections have an open arrowhead, and non-detections have dashed arrow. The transitions are labeled with the wavelength in  $\mu\text{m}$ .

We observe *more* H<sub>2</sub>O than OH, suggesting that high-temperature chemistry was operative long enough to leave a lasting effect on the chemistry of this gas.

The detection of OH, with an abundance only 7 times less than that of H<sub>2</sub>O, disagrees with theoretical models for C shocks, which predict nearly complete conversion of OH into H<sub>2</sub>O. This suggests either (1) the H<sub>2</sub>O abundance is underestimated due to beam-dilution, (2) we are observing OH and H<sub>2</sub>O from different types of shocks in regions with a range of pre-shock densities, or (3) the models are not appropriate for the molecular shocks in 3C 391. We detected bright ionic lines (including [O III] and [N III]) that are only expected from dissociative shocks, so we know that a range of shocks is present within our beam. However, the infrared OH line ratios are consistent with coming from a region with the same physical conditions as inferred from the infrared H<sub>2</sub>O, millimeter-wave CS, and radio-wave OH maser lines. The disagreement between observations and predictions is at least partially due to the fact that the models are for non-dissociative shocks (Kaufman and Neufeld 1996). Including the effects of photodissociation of H<sub>2</sub>O by the interstellar radiation field—as well as radiation local to the remnant—could produce OH in the abundance we observe (Lockett, Gauthier, & Elitzur 1998).

The water abundance we derive for 3C 391:BML is significantly lower than that observed from molecular shocks in HH 54 (Liseau et al. 1996) or Orion (Harwit et al. 1998). In particular, in the Orion BN-KL region, the H<sub>2</sub>O abundance is  $[H_2O/H_2] \simeq 5 \times 10^{-4}$  (Harwit et al. 1998), incorporating nearly all of the oxygen in the gas. The difference between the Orion BN-KL shock and the 3C 391:BML shock could be due to limited angular resolution: 3C 391 is about 20 times further away than Orion, while the angular resolution of our observations is the same as that of Harwit et al. (1998). The difference could also be due to details of the interaction between the energetic events (a steady stellar wind in Orion *vs.* impulsive supernova shock in 3C 391) and the interstellar medium (a molecular cloud and H II region in Orion *vs.* a giant molecular cloud with no H II region in 3C 391).

## 5. Conclusions

For the first time, thermal emission from the lower energy-levels of H<sub>2</sub>O and OH were detected from a supernova remnant. The emission arises from gas cooling behind a shock front that is impinging a particularly dense clump in the parent molecular cloud; this site is called 3C 391:BML (broad molecular line). Our spectra of interaction sites in W 44 and W 28 did not reveal OH or H<sub>2</sub>O emission, although CO emission and OH (foreground) absorption were detected. 3C 391 is not a unique case of a supernova remnant-molecular cloud interaction, but the infrared molecular lines imply the presence of higher-density clumps than near W 44 and W 28, similar to IC 443. Together with outflows from young stars, supernova remnants are energetic events capable of altering cloud chemistry and producing substantial columns of H<sub>2</sub>O and OH. Supernova-molecular cloud interactions are probably common, and they have been suggested as an explanation for a new class of mixed-morphology X-ray and radio supernova remnants (Rho & Petre 1998). We can expect substantial advances in understanding shock-induced chemistry in supernova-molecular cloud interactions by using future observatories capable of higher angular and spectral resolution in the far-infrared, such as planned for SOFIA (Erickson 1995) and FIRST (Poglitsch 1998), where we will better resolve the fast and slow shocks into gas of varying pre-shock density, and we will better resolve a larger number of spectral lines from each molecule.

The observations that we describe in this paper are part of the *ISO* open time granted to U.S.

astronomers thanks to cooperation between the ESA and NASA. The research described in this paper was carried out in part by the California Institute of Technology, under a contract with the National Aeronautics and Space Administration.

## REFERENCES

Bergin, E. A., Langer, W. D., & Goldsmith, P. F. 1995, *ApJ*, 442, 222

Cernicharo, J., Lim, T., Cox, P., Gonzalez-Alfonso, E., Caux, E., Swinyard, B. M., Martin-Pintado, J., Baluteau, J. P., & Clegg, P. 1997, *A&A*, 323, L25

Clegg, P. E., et al. 1996, *A& A*, 315, L38

Draine, B. T., Roberge, W. G., & Dalgarno, A. 1983, *ApJ*, 264, 485

Frail, D. A., Goss, W. M., Reynoso, E. M., Giacani, E. B., Green, A. J., Otrupcek, R. 1996, *AJ*, 111, 1651

Elitzur, M. 1976, *ApJ*, 203, 124

Erickson, E. F. 1995, *Space Sci. Rev.* 74, 91

Graff, M. M., & Dalgarno, A. 1987, *ApJ*, 317, 432

Green, A. J., Frail, D. A., Goss, W. M., & Otrupcek, R. 1997, *AJ*, 114, 2058

Green, S., Maluendes, S., & McLean, A. D. 1993, *ApJS*, 85, 181

Harwit, M., Neufeld, D. A., Melnick, G. J., & Kaufman, M. J. 1998, *ApJL*, 497, L105

Hollenbach, D. J., and McKee, C. F. 1989, *ApJ*, 355, 197

Irvine, W. M., Goldsmith, P. F., & Hjalmarson, Å 1987, in *Interstellar Processes*, eds. D. J. Hollenbach & H. A. Thronson, Jr. (Dordrecht: Reidel), p. 561.

Kaufman, M. J., & Neufeld, D. A. 1996, *ApJ*, 456, 611

Kessler, M. F. et al. 1996, *A& A*, 315, L27

Liseau, R. et al. 1996, *A& A*, 315, L181

Lockett, P., Gauthier, E., & Elitzur, M. 1998, *ApJ*, submitted

McKee, C. F., and Hollenbach, D. J., 1979, *ApJS*, 41, 555

Offer, A. R., van Hemert, M. C., & van Dishoeck, E. F. 1994, *J. Chem. Phys.* 100, 362

Pickett, H. M. Poynter, R. L., Cohen, E. A., Delitsky, M. L., Pearson, J. C., & Müller, H. S. P. 1996, *Submillimeter, Millimeter, and Microwave Spectral Line Catalog: Revision 4*, JPL publication 80-23, (Pasadena: JPL)

Poglitsch, A. 1998, in *The Far-Infrared and Submillimeter Universe* (ESA SP-401), eds. G. Pilbratt, S. Volonte, & A. Wilson (ESA: Noordwijk), in press

Reach, W. T., & Rho, J.-H. 1996, *A& A*, 315, L277 (paper I)

Reach, W. T., & Rho, J.-H. 1998, ApJ, submitted

Rho, J.-H., Petre, R., 1998, ApJL, 503, L167

Sternberg, A., & Dalgarno, A. 1995, ApJS, 99, 565

van Dishoeck, E. F., & Black, J. H. 1986, ApJS, 62, 109

Wagner, A. F., & Graff, M. M. 1987, ApJ, 317, 423

Wilner, D. J., Reynolds, S. P., Moffett, D. A. 1998, AJ, 115, 247

Wootten, A. 1977, ApJ, 216, 440

Wootten, A. 1981, ApJ, 245, 105